(54) J. A. Jaecker, W. R. Robinson, and R. A. Walton, *J. Chem. Soc., Chem. Commun.*, 306 (1974).
(55) J. A. Jaecker, W. R. Robinson, and R. A. Walton, *Inorg. Nucl. Chem. Lett.*, **10**, 93 (1974).
(56) A. Davison and D. L. Reger, *J. Am. Chem. Soc.*, **94**, 9237 (1972); M. L. H. Green, L. C. Mitchard, and M. G. Swanwick, *J. Chem. Soc. A*, 794 (1971).
(57) D. J. Cardin, B. Cetinkaya, and M. F. Lappert, *Chem. Rev.*, **72**, 545 (1972); F. A. Cotton and C. M. Lukehart, *Prog. Inorg. Chem.*, **16**, 487 (1972).

Contribution from the Departments of Chemistry, University of Windsor, Windsor, Ontario N9B 3P4, Canada, and Lewis University, Lockport, Illinois 60441

Phosphine–Borane Derivatives. 9. Vibrational Spectra of the Trimethylphosphine Adducts of Boron Trihalides

JOHN E. DRAKE,* J. LAWRENCE HENCHER, and BERNARD RAPP

Received December 28, 1976 AIC60910Z

The IR and Raman spectra of $Me_3P{\cdot}BCl_3$, $Me_3P{\cdot}BBr_3$, and $Me_3P{\cdot}BI_3$ are reported. A normal-coordinate analysis, utilizing a modified Urey–Bradley force field, supports the assignments. The values of K_{PB} obtained using this modified force field are consistent with the increase in relative Lewis acidity along the series $BCl_3 < BBr_3 < BI_3$. In all of the adducts, the P–B force constant is larger than in the corresponding $PH_3{\cdot}BX_3$ species.

One feature of studies of the vibrational properties of adducts containing the P–B bond has been the wide range of assigned P–B stretching frequencies.[1-5] Furthermore, significantly different values have been assigned to the magnitude of the P–B stretching force constant.[5-9] In our recent vibrational spectroscopic investigation of the $PH_3{\cdot}BX_3$ adducts,[6] we obtained reasonable agreement in the assignment of the P–B stretching mode and its corresponding force constant with that of an independently conducted study.[9] The values of the force constant vary only slightly from adduct to adduct. The relatively weak donor properties of phosphine as a Lewis base have prompted us to extend our investigation to the BX_3 (X = Cl, Br, I) adducts of progressively methyl-substituted phosphine in order to ascertain the effects of such substitution on the magnitude of the P–B force constant. (Our own ^{11}B NMR study of this adduct series[10] as well as that of Cowley and Damasco[11] on the adduct series $Me_{3-n}PH_n{\cdot}BH_3$ seems to indicate an increasing PB interaction with increasing donor strength.)

Of the various methyl-substituted phosphines, Me_3P was chosen as the appropriate base in this investigation because of its apparently superior donor properties[12] and because of the relative structural simplicity of its BX_3 adducts. These advantages should facilitate a conclusive vibrational assignment for the adduct series which will assist in our analysis of the partially methyl-substituted phosphine adducts of the boron trihalides.

Experimental Section

Starting Materials. Trimethylphosphine was prepared according to the method of Markham et al.[13] from the reaction of MeLi (Alfa Inorganics, Beverly, Mass.,) with PCl_3 (Anachemia, Toronto) in an ethereal solution. The product was checked for purity by vapor pressure measurement (160 mm at 0 °C; lit. 161.0 mm, 158 mm[14] at 0 °C) and by ^1H NMR spectrum.[15] The IR[16] and Raman[17,18] spectra were found to agree with those previously published. The boron trihalides were purified and checked in the manner reported previously.[19]

Formation of the Adducts. All reactions were carried out on a conventional Pyrex-glass vacuum system, employing the same type of reaction vessels and methods of addition with the trimethylphosphine systems as in our previous work with the phosphine–boron trihalide adducts.[6]

Spectroscopic Techniques. Raman spectra were recorded on both solid and solution samples of the adducts. Equipment type and employment were the same as in our previous study[6] except that CH_2Br_2 replaced MeI as one of the two solvents for the solution spectra of the adducts. It was found that methylene bromide had no Raman bands in the CH symmetric stretching and bending regions of the adducts, thus allowing us to obtain polarization data in these areas.

The IR spectra were recorded on both solid and solution samples of the adducts, using methods and equipment as previously reported.[6]

* To whom correspondence should be addressed at the University of Windsor.

Table I. Description of Vibrational Assignments for $Me_3P{\cdot}BX_3$ Adducts[a] $\Gamma_v = 10\ A_1 + 5\ A_2 + 15\ E$

A_1	A_2	E	
ν_1	ν_{11}	ν_{16}, ν_{17}	CH_3 d str
ν_2		ν_{18}	CH_3 s str
ν_3	ν_{12}	ν_{19}, ν_{20}	CH_3 d def
ν_4		ν_{21}	CH_3 s def
ν_5	ν_{13}	ν_{22}, ν_{23}	CH_3 rock
ν_6			PB str
ν_7		ν_{24}	CP str
ν_8		ν_{25}	BX str
ν_9		ν_{26}	PC_3 def
		ν_{27}	PC_3 rock
ν_{10}		ν_{28}	BX_3 def
		ν_{29}	BX_3 rock
	ν_{14}	ν_{30}	CH_3 torsion
	ν_{15}		Frame torsion

[a] Descriptions of CH_3 modes are based on the local symmetry. Key: d, degenerate; s, symmetric.

Discussion

The molecules $Me_3P{\cdot}BX_3$ are assumed to be of C_{3v} symmetry in staggered conformation leading to 45 fundamental vibrations for which the conventional descriptions are given in Table I. The A_1 and E modes are active in both IR and Raman regions but the A_2 modes are inactive in both spectra and were not observed. The A_1 modes are polarized and the E modes depolarized in the Raman effect.

For comparison purposes, the values of the assigned and calculated frequencies for the three adducts are given in Table II.[20] Tables III–V provide the complete spectroscopic information on each adduct, together with the respective potential energy distributions.

(1) The Methyl Group Vibrations: ν_1–ν_5; ν_{16}–ν_{23}. By use of the previously assigned methyl group fundamental modes for Me_3P,[18] no difficulty was encountered in making the analogous assignments in the Me_3P adducts. Consistent with a previous investigation of $Me_3P{\cdot}BH_3$[21] all stretching modes are observed at higher wavenumber in the adducts than in the pure base. There is a general trend in these frequencies toward

Table III. Observed IR and Raman Frequencies/cm^{-1}, ±3 cm^{-1}, for $Me_3P{\cdot}BCl_3$, with Potential Energy Distributions

Assignment	IR (Nujol mull)	Raman (solid)	Raman (soln)[a]	PED[c]
$\nu_1, \nu_{11}, \nu_{16}, \nu_{17}$		3002 m		$101f_{CH^2} - 1f_{CH/CH'}$
ν_2, ν_{18}		2924 s	2925 vs, p	$98f_{CH^2} + 2f_{CH/CH'}$
$2\nu_3, 2\nu_{19}, 2\nu_{20}$		2832 w 2803 w	2840 m, p	
$\nu_3, \nu_{12}, \nu_{19}, \nu_{20}$	1416 s	1415 m		$79f_{HCH^2} + 8f_{HCP^2} + 13f_{HCP/HCP'}$
ν_{21}	1304 s	1310 w		$43f_{HCH^2} + 63f_{HCP^2} + 9f_{CP^2} - 15f_{HCP/HCP'}$
ν_4	1296 s			
ν_{13}, ν_{22}	992 s	983 vw	ca. 980 w, dp?	$6f_{HCH^2} + 86f_{HCP^2} + 1f_{HCP/HCP'} + 3f_{CP^2}$
ν_5, ν_{23}	959 s	949 vw		$6f_{HCH^2} + 92f_{HCP^2} + 1f_{HCP/HCP'}$
$\nu_7 + \nu_{27}$	861 w	865 w		
ν_6 (^{10}B)	801 m	800 vw		
ν_6	772 s	773 s	756[b] w, p	$55K_{PB} + 12K_{BX} + 10H_{PBX} + 6H_{XBX} + 6f_{CP^2}$
ν_{24}	738 s	745 w	741[b] vw, dp?	$9f_{CPB^2} + 9f_{CP^2} + 57K_{BX} + 14H_{PBX} + 7H_{XBX} - 3f_{CP/BX}$
ν_{25}	710 vs	715 w	710[b] vw, dp?	$8f_{HCP^2} + 82f_{CP^2} + 8K_{BX} - 7f_{CP/CP'} + 4f_{CP/BX}$
$\nu_8 + \nu_9$		700 w		
ν_7	664 s	663 s	662 m, p	$7f_{HCP^2} + 63f_{CP^2} + 11f_{CP/CP'}$
ν_8	395 m	399 vs	398 m, p	$8K_{PB} + 34K_{BX} + 35F_{XX} + 12F_{PX}$
ν_9	300 m	298 s	296[b] w, p?	$22f_{CPC^2} + 20f_{CPB^2} + 13H_{PBX} + 8H_{XBX} + 23F_{XX} + 10F_{PX} - 5f_{CPB/CPB'}$
ν_{26}	275 w	269 m sh		$19f_{CPC^2} + 11f_{CPB^2} + 16K_{BX} + 9H_{PBX} + 23F_{XX} + 12F_{PX}$
ν_{28}	250 w	248 m	248[b] m, dp?	$60f_{CPC^2} + 10H_{XBX} + 25F_{XX}$
ν_{27}		203 s, br	205 m, dp?	$16f_{CPC^2} + 24f_{CPB^2} + 10H_{PBX} + 14H_{XBX} + 20F_{XX} + 9F_{PX} + 3f_{CPB/CPB'}$
		172 vw, br		
ν_{10}		160 w, sh	161 w, p	$30f_{CPC^2} + 28f_{CPB^2} + 12K_{PB} + 8H_{PBX} + 16F_{PX} - 6f_{CPB/CPB'}$
ν_{29}		142 w, br	140 vw, dp?	$44f_{CPC^2} + 31H_{PBX} + 18F_{PX} + 5f_{CPB/CPB'}$

[a] Spectrum in CH_2Cl_2. [b] In CH_2Br_2. Key: sh, shoulder; br, broad. [c] Contributions greater than 5% except for significant interactions.

decreasing values along the adduct series with $BCl_3 > BBr_3 > BI_3$. The frequencies of the deformation modes remain essentially unchanged, while those of the rocking modes are again higher in the adducts than in the free phosphine donor. Unlike the stretching frequencies, however, the values assigned to the methyl rocking modes show no significant trend within the adduct series.

(2) The PC_3 Modes: ν_7, ν_9; ν_{24}, ν_{26}, ν_{27}. By comparison with the previously assigned PC_3 group frequencies for trimethylphosphine,[17] the symmetric stretching and deformation modes were expected in the 650- and 300-cm^{-1} regions, respectively. In all three adducts, vibrational bands, polarized in the Raman region (see Tables III–V), are observed in these areas and with only relatively small changes in vibrational frequency in the symmetric modes between donor and adduct series.

Similarly, Raman depolarized bands were expected in the spectra of the adducts in the vicinity of 700 and 260 cm^{-1} corresponding to the degenerate, asymmetric PC_3 stretch and deformation in trimethylphosphine. In both the tribromide and triiodide adducts, these bands are easily located and assigned. Both modes appear at slightly higher values in the adducts (ca. 35 cm^{-1} for ν_d and 20 cm^{-1} for δ_d). The assignment of these two bands in the trichloride adduct is complicated by the close proximity of others which, in the light of our previous work on $PH_3{\cdot}BCl_3$,[6] are attributable to BCl_3 vibrational activity (see Figures 1 and 2). Both the 715- and the 745-cm^{-1} (738 cm^{-1} in the IR region) bands are depolarized in the Raman region. The assignment of the higher frequency band to the PC_3 asymmetric stretch, ν_{24}, is preferred because of internal consistency with the straightforward assignments made for the other two adducts. Furthermore, the 715-cm^{-1} band has a comparable position, along with its symmetric counterpart (395 cm^{-1}), in the $PH_3{\cdot}BCl_3$ spectrum (730 and 399 cm^{-1}, respectively). The small feature near 700 cm^{-1} seems to be polarized in the Raman spectrum of the adduct in CH_2Br_2 solution and may be an addition band (Table III).

The presence of BCl_3 vibrational activity also causes difficulty in assigning the PC_3 asymmetric deformation frequency in $Me_3P{\cdot}BCl_3$. Two bands are observed in the 250-cm^{-1} region of the adduct spectrum, one at 248 cm^{-1} and the other as a shoulder at 269 cm^{-1}. The PC_3 asymmetric deformation mode is assigned to the latter band. This is consistent with the previous assignment of ν_{26} for the other adducts (and with our earlier work with $PH_3{\cdot}BCl_3$[6] where $\delta_d(BCl_3)$ was located at 244 cm^{-1}).

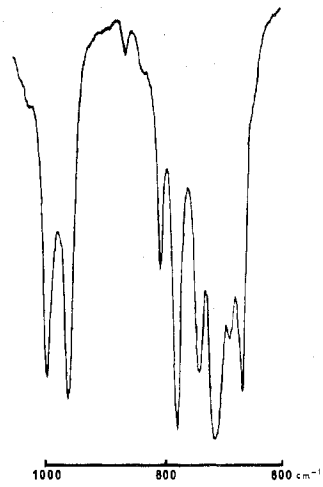

Figure 1. IR spectrum of $Me_3P{\cdot}BCl_3$, Nujol mull (1000–600 cm^{-1}).

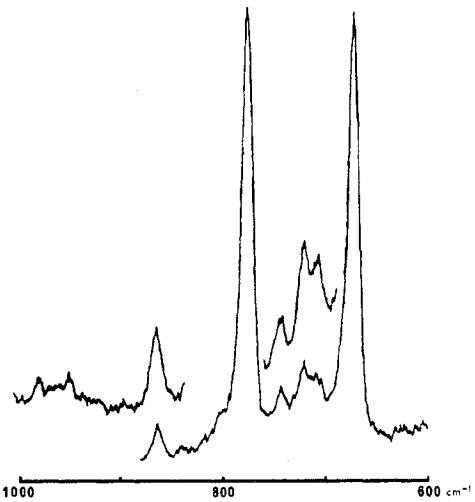

Figure 2. Raman spectrum of solid $Me_3P{\cdot}BCl_3$ (1000–600 cm^{-1}).

Table IV. Observed IR and Raman Frequencies/cm^{-1}, ±3 cm^{-1}, for $Me_3P{\cdot}BBr_3$, with Potential Energy Distributions

Assignment	IR (Nujol)	Raman (solid)	Raman (soln)[a]	PED[c]
$\nu_1, \nu_{11}, \nu_{16}, \nu_{17}$		2996 s		
ν_2, ν_{18}		2921 vs	2922[b] s, p	
$2\nu_3, 2\nu_{19}, 2\nu_{20}$		2800 w		
$2\nu_4$		2570 w		
$\nu_3, \nu_{12}, \nu_{19}, \nu_{20}$	1410 w	1408 m		
ν_{21}	1299 w	1311 w		See Table III
ν_4	1291 w	1300 w	1275[b] m, p	
ν_{13}, ν_{22}	983 s	980 vw	980[b] w, p	
ν_5, ν_{23}	953 s	959 vw	960 w, dp	
$\nu_7 + \nu_{27}$	864 w	850 w		
ν_6 (^{10}B)	785 sh	785 w sh		
ν_6	765 m	765 m 755 m	775[b] p	$8f_{HCP^2} + 16f_{CP^2} + 52K_{PB}$
ν_{24}	730 m	727 w		$10f_{HCP^2} + 73f_{CP^2}$
ν_{25} (^{10}B)	670 sh	675 w sh	680 vw, dp?	
ν_7	652 s	653 m	652 m, p	$54f_{CP^2} + 14K_{PB} + 12f_{CP/CP'}$
ν_{25}	621 vs	626 615 m		$10f_{CPB^2} + 19f_{CP^2} + 45K_{BX} + 8H_{PBX} + 10H_{XBX}$
ν_9	325 w	321 m	321 m, p	$30f_{CPC^2} + 31f_{CPB^2} + 12K_{BX} + 7F_{XX} + 17F_{PX} - 15f_{CPB/CPB'}$
ν_{26}		280 m	280[b] w, dp	$86f_{CPC^2}$
ν_8		232 m	231 s, p	$10f_{CPC^2} + 10f_{CPB^2} + 18K_{BX} + 59F_{XX} - 5f_{CPB/CPB'}$
ν_{27}		219 w		$7f_{CPC^2} + 46f_{CPB^2} + 23K_{BX} + 7F_{PX} + 11f_{CPB/CPB'}$
ν_{28}		171 m	165 w, dp	$23H_{XBX} + 67F_{XX}$
ν_{10}		145 m	141 w, p	$23f_{CPC^2} + 24f_{CPB^2} + 11K_{PB} + 8H_{PBX} + 9H_{XBX} + 21F_{PX} + 13F_{XX} - 12f_{CPB/CPB'}$
ν_{29}		104 m		$10f_{CPB^2} + 41H_{PBX} + 41F_{PX}$

[a] Spectrum in CH_2Cl_2. [b] In CH_2Br_2. [c] Contributions greater than 5%.

Table V. Observed IR and Raman Frequencies/cm^{-1}, ±3 cm^{-1}, for $Me_3P{\cdot}BI_3$, with Potential Energy Distributions

	IR (Nujol)	Raman (solid)	Raman (soln)[a]	PED[c]
$\nu_1, \nu_{11}, \nu_{16}, \nu_{17}$		2987 s		
ν_2, ν_{18}	2910 w	2912 vs	2920 m, p	
$2\nu_3, 2\nu_{19}, 2\nu_{20}$		2800 w		
$\nu_3, \nu_{12}, \nu_{19}, \nu_{20}$	1411 w	1409 m		
ν_{21}	1315 w	1314 w		See Table III
ν_4	1299 w	1299 w	1300 p	
ν_{13}, ν_{22}	985 sh	997 w	999 m, p	
ν_5, ν_{23}	957 s	953 w		
ν_6	758 s	760 s	763[b] w, p	$11f_{HCP^2} + 24f_{CP^2} + 49K_{PB}$
ν_{24}	738 sh	737 s	748[b] w, dp?	$12f_{HCP^2} + 80f_{CP^2} - 8f_{CP/CP'}$
ν_7	650 m	654 646 m	653 w, p	$45f_{CP^2} + 32K_{PB} + 9f_{CP/CP'}$
ν_{25} (^{10}B)	580 sh	580 m	585 w, dp	
ν_{25}	565 s	556 s	567 m, dp	$25f_{CPB^2} + 11f_{CP^2} + 36K_{BX}$
ν_9		309 w	307[b] vw, p?	$38f_{CPC^2} + 51f_{CPB^2} + 9F_{PX} - 15f_{CPB/CPB'}$
ν_{26}		277 w		$90f_{CPC^2}$
ν_{27}		213 w		$47f_{CPB^2} + 30K_{BX} + 9f_{CPB/CPB'}$
ν_8		191 s	190 s, p	$19K_{BX} + 65F_{XX}$
ν_{28}		129 m	132 vw, dp	$83F_{XX}$
ν_{10}		112 s	111 vw, p	$13H_{PBX} + 12H_{XBX} + 42F_{XX} + 34F_{PX} - 23f_{PBX/PBX'}$
ν_{29}		84 m	84[b] w, dp	$23H_{PBX} + 40F_{PX} + 21f_{PBX/PBX'}$

[a] Spectrum in CH_2Cl_2. [b] In CH_2Br_2. [c] Contributions greater than 5%.

The PC_3 rocking modes, ν_{27}, are assigned to the medium-strength, somewhat depolarized bands at 219 and 213 cm^{-1} in the spectrum of the bromide and iodide adducts, respectively. (This region is relatively clear of BX_3 vibrational activity.) With these assignments as a model, the 203-cm^{-1} frequency is assigned to ρ_{PC_3} for the chloride adduct. The unexpectedly lower frequency for this mode implies a considerable degree of mixing with the 248-cm^{-1} band, $\delta_d(BCl_3)$, previously mentioned. This conjecture is borne out in the normal-coordinate analysis.

(3) The Phosphorus–Boron Stretching Frequency: ν_6. The spectra of all three adducts exhibit a band in the vicinity of 760 cm^{-1} which is polarized in the Raman and strong in both the IR and Raman effect. No other symmetric modes remain to be assigned in this region. Accordingly, the PB stretching mode is assigned to the bands at 773, 765, and 760 cm^{-1} in the Me_3P adducts of BCl_3, BBr_3, and BI_3, respectively. Very weak shoulders were observed at 800 and 785 cm^{-1} on the major bands in the spectra of the first two adducts. Nothing comparable was seen in the spectrum of the BI_3 adduct. That these weak signals may be attributed to the ^{10}BP stretch is supported by the calculations.

(4) The BX_3 Modes: ν_8, ν_{10}; ν_{25}, ν_{28}, ν_{29}. In assigning the various BX_3 fundamental vibrations, considerable reliance was placed on our previous work[6] as well as on other vibrational studies of BX_3 adducts.[22-24]

The assignment of the BX_3 symmetric stretch was straightforward in the spectra of all three adducts. The Raman bands are intense and strongly polarized. Their positions are consistently lower than the corresponding mode in the spectra of the free boron trihalides,[25] a feature which has been noted for other BX_3 adducts.[22,23] Relative to the analogous $PH_3{\cdot}BX_3$ system[6] the position of $\nu_s(BCl_3)$ remains virtually unchanged, while its location is some 40 cm^{-1} lower in the spectra of the

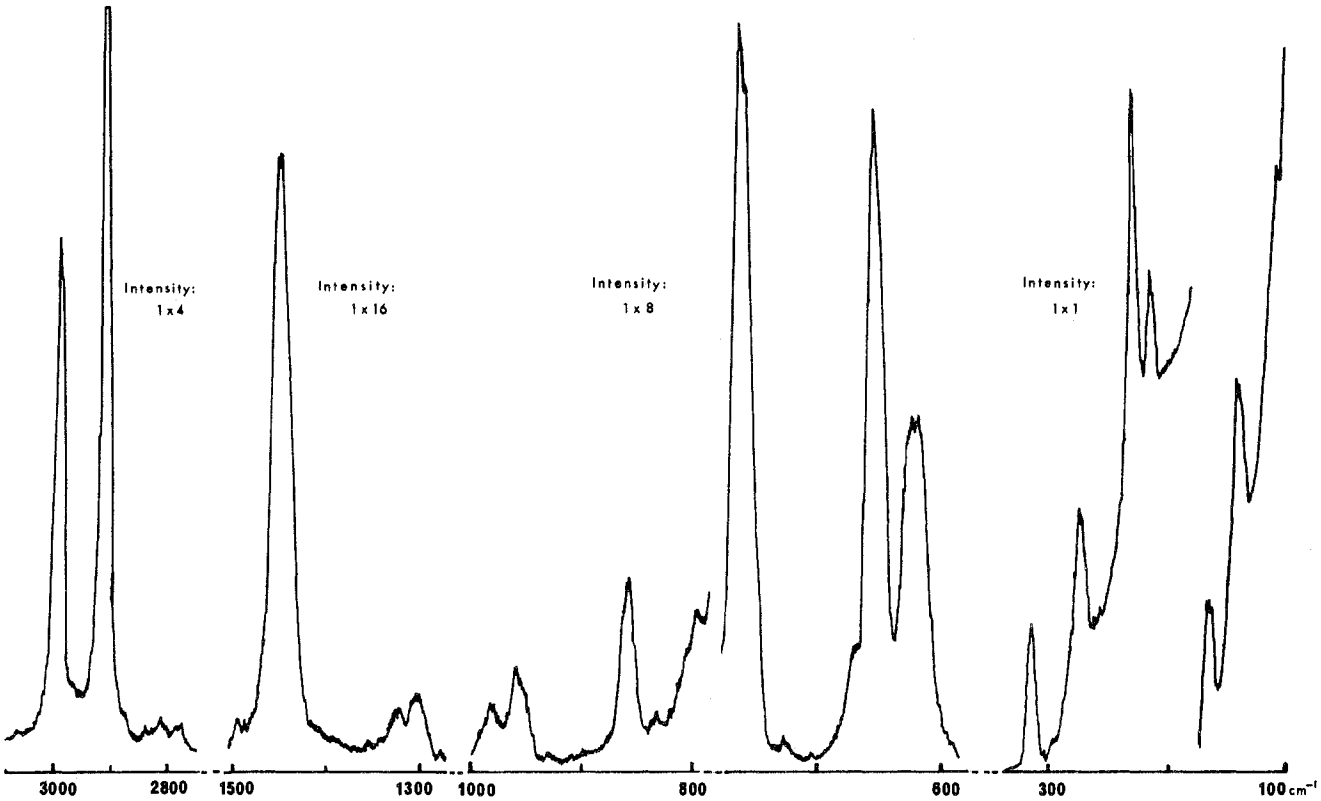

Figure 3. Selected regions of the Raman spectrum of solid $Me_3P{\cdot}BBr_3$.

other two adducts. All of the asymmetric BX_3 stretching frequencies exhibit the expected descending values from the chloride to the iodide, with the magnitudes notably lower than in the phosphine adducts, except for the chloride where the difference is only about 15 cm^{-1}. The rationale for assigning ν_{25} at 715 cm^{-1} in the chloride has been given in an earlier section. In the bromide this vibrational mode is assigned to the split peak centered at 620 cm^{-1} in the Raman spectrum of the solid adduct (Figure 3). It is unfortunate that this peak was obscured by solvent activity in the solution studies, thereby precluding polarization data. However, the broadness of the peak as well as the splitting can be interpreted as evidence of an E-type mode.[26] In the Raman solution spectrum of $Me_3P{\cdot}BI_3$, the depolarized band at 556 cm^{-1} is assigned to ν_{25}.

Except for the chloride compound, the BX_3 deformation bands occur in relatively close proximity to one another. The symmetric deformation modes are assigned to polarized Raman bands at 160, 145, and 112 cm^{-1}, respectively; these are all shifted to considerably lower wavenumbers than in the spectra of their phosphine counterparts. The asymmetric mode is, in each case, higher than the symmetric. This order is consistent with our earlier findings[6] as well as with the observations of others on similar boron trihalide adducts.[21-23] The arguments for assigning the 248-cm^{-1} band to ν_{28} in the spectrum of the BCl_3 adduct have already been given in a previous section. The depolarized Raman bands at 171 and 129 cm^{-1} are assigned to this mode in the bromide and iodide spectra, respectively.

The BX_3 rocking mode, ν_{29}, is observed as the lowest frequency fundamental and is assigned without difficulty (Table II).[20] Rather good agreement was observed between these values and our earlier investigation.[6] Again, the BCl_3 rocking mode exhibited about the same vibrational frequency as in $PH_3{\cdot}BCl_3$, while those of the bromide and iodide were about 10 cm^{-1} lower.

Normal-Coordinate Analysis. The force constants were calculated from the above frequency assignments, using our own computer program[27] which obtains the normal coordinates in terms of the mass-weighted Cartesian coordinates.[28]

As a prelude to analysis of the $Me_3P{\cdot}BX_3$ adducts, the calculations for Me_3P were repeated, using the frequency assignments of Bouquet and Bigorgne[18] and the observed structural parameters reported by Bartell and Brockway.[29] When the H-atom coordinates were explicitly included in the analysis, the interaction constant $f_{CP/CP'}$ was 0.20 mdyn $Å^{-1}$ in contrast to the value −0.034 mdyn $Å^{-1}$ obtained when the methyl group was treated as an effective mass. In view of this rather large difference we decided to include the H-atom coordinates in the subsequent analysis of the adducts. The force constants are given in Table VI.

In the analysis of the $Me_3P{\cdot}BX_3$ complexes, C_{3v} symmetry was assumed. The molecular structures were based on those of $Me_3P{\cdot}BH_3$[30] and the $Me_3N{\cdot}BX_3$ adducts.[22] Since no torsional frequencies were observed, all torsional coordinates were excluded from the analysis. The assumed structures are given in Table VI.

The methyl group modes were found to be well treated with the force constants f_{CH^2}, $f_{CH/CH'}$, f_{HCH^2}, f_{HCP^2}, and $f_{HCP/HCP'}$. No further attempt was made to reproduce the partially observed splitting in the CH_3 rocking frequencies ν_5, ν_{13}, ν_{22}, and ν_{23}.

Apart from the unobserved torsional frequencies, only 11 $C_3P{\cdot}BX_3$ modes remained as observables. After mandatory selection of the seven diagonal force constants, this meant that only four interaction constants could be uniquely determined. By trial and error it was found that the combination of the interaction constants $f_{CP/CP'}$ and $f_{CPB/CPB'}$ and the Urey–Bradley nonbonded repulsion constants[31] F_{XX} and F_{PX} reproduced the observed frequencies very well. In the cases of the chloride and the iodide, additional interaction constants were included, which only contributed to two normal modes and had no apparent effect on the other force constants.

The potential energy distributions are given in Tables III–V and the force constants are given in Table VI. In order to facilitate comparisons with the results for other adduct systems, the nonzero elements of the F matrix are given in Table VII.

Table VI

	Me_3BX_3			
	X = Cl	X = Br	X = I	Me_3P
Modified Urey-Bradley Force Fields for $Me_3P{\cdot}BX_3$ and Me_3P[a]				
f_{CH^2}[b]	4.800 (5)	4.782 (1)	4.756 (7)	4.686 (4)
f_{HCH^2}	0.436 (1)	0.433 (1)	0.438 (2)	0.511 (1)
f_{HCP^2}	0.648 (2)	0.640 (2)	0.639 (4)	0.555 (2)
f_{CPC^2}	0.64 (3)	0.81 (7)	0.82 (1)	1.03 (1)
f_{CPB^2}	0.60 (20)	0.84 (3)	0.99 (17)	
f_{CP^2}	3.10 (4)	3.13 (2)	3.32 (3)	3.13 (2)
K_{PB}	1.85 (9)	1.917 (16)	2.22 (5)	
K_{BX}	1.44 (7)	0.96 (3)	0.60 (4)	
H_{PBX}	0.63 (17)	0.42 (4)	0.22[c]	
H_{XBX}	0.37 (13)	0.44 (3)	0.20[c]	
F_{XX}	0.53 (9)	0.61 (1)	0.66 (2)	
F_{PX}	0.26 (13)	0.25 (3)	0.18 (2)	
$f_{CH/CH'}$	0.045 (3)	0.045 (3)	0.045 (3)	0.045 (3)
$f_{HCP/HCP'}$	−0.120 (4)	−0.109 (4)	−0.107 (4)	−0.070 (2)
$f_{CP/CP'}$	0.28 (3)	0.34 (3)	0.36 (3)	0.20 (3)
$f_{CPB/CPB'}$	−0.02 (8)	−0.06 (8)	−0.045 (8)	
$f_{CP/BX}$[d]	−0.15[c]			
$f_{CPC/CPC'}$				0.27
$f_{PBX/PBX'}$			−0.19 (3)	
Structural Parameters[e]				
r(P–B)	1.901	1.901	1.901	
r(B–X)	1.84	2.02	2.265	
r(C–P)	1.819	1.819	1.819	1.846 (3)
r(C–H)	1.08	1.08	1.08	1.091 (6)
α(PBX)	109.5	109.5	109.5	
α(HCP)	109.5	109.5	109.5	110.7 (5)
α(CPC)	105.4	105.4	105.4	98.6 (3)

[a] Stretching constants in 10^5 dyn cm^{-1}, bending constants in 10^{-11} ergs rad^{-2} and stretch/bend interaction constants in 10^{-5} dyn rad^{-1} (uncertainties in parentheses). [b] General valence force constants f_{ij}; Urey-Bradley force constants K(stretch), H(bend), and F(repulsion). Linear constant $F' = -(1/10)F$ assumed. [c] Given fixed value in least-squares analysis. [d] This is the interaction between CP and BX which are trans to each other. [e] Bond lengths in A (=100 pm) and angles in degrees.

Table VII. Nonzero Elements of the F Matrix[a] for Frame Coordinates, $C_3P{\cdot}BX_3$

	$Me_3P{\cdot}BCl_3$	$Me_3P{\cdot}BBr_3$	$Me_3P{\cdot}BI_3$	Me_3P
CP	3.10	3.13	3.32	3.13
PB	2.35	2.37	2.52	
BX	2.27	1.89	1.58	
CPC	0.64	0.81	0.81	1.02
CPB	0.59	0.84	1.08	
XBX	1.08	1.43	1.55	
PBX	0.98	0.80	0.52	
PB/BX	0.18	0.17	0.11	
BX/BX'	0.38	0.44	0.47	
PB/PBX	0.21	0.20	0.15	
BX/PBX	0.21	0.22	0.17	
BX/XBX	0.40	0.53	0.64	
CP/BX[b]	−0.15			
CP/CP'	0.28	0.34	0.36	0.20
CPB/CPB'	−0.07	−0.21	−0.18	
CPC/CPC'				0.27
PBX/PBX'			−0.19	

[a] Stretching constants in 10^5 dyn cm^{-1}; bending in 10^{-11} ergs radi^{-2}; stretch/bend interaction in 10^{-5} dyn rad^{-1}. [b] See Table VI, footnote *b*.

The good agreement between the observed and calculated frequencies and the apparently smooth trends of the force constants in the sequence Cl, Br, I indicate that the force field is a reasonable one.

In the course of the present work we noted that the potential energy distributions given for $PH_3{\cdot}BBr_3$ and $PH_3{\cdot}BI_3$ in our earlier paper[6] are not consistent with our assignment of the BX_3 rocking frequencies of these molecules. The force constants recalculated using the corrected assignment together with the previously obtained values of $PH_3{\cdot}BCl_3$ are given in Table VIII. Although the force constants were altered considerably by this change in assignment, the new values are more consistent with the present results for $Me_3P{\cdot}BX_3$ and, at the same time, leave unchanged the qualitative conclusions that were drawn about the trend in PB bond strength.

Table VIII. Modified Urey-Bradley Force Field for $PH_3{\cdot}BX_3$[a]

	X = Cl	X = Br	X = I
K_{PH}	3.38 (1)[b]	3.328 (3)	3.246 (2)
K_{PB}	1.23 (8)	1.74 (2)	1.92 (1)
K_{BX}	1.74 (5)	1.50 (2)	1.11 (1)
H_{HPH}	0.492 (6)	0.495 (1)	0.491 (1)
H_{HPB}	0.42 (1)	0.408 (5)	0.438 (2)
H_{PBX}	0.01 (7)	0.11	0.06
H_{XBX}	0.3 (1)	0.3 (1)	0.21
F_{XX}	0.54 (8)	0.47 (2)	0.54 (1)
F_{PX}	0.32 (8)	0.226 (8)	0.174 (6)
$f_{HPB/PB}$	−0.114[c]	−0.081 (9)	−0.011 (8)
$f_{XBX/PBX}$	−0.14[c]	0[c]	0.065 (6)

[a] K, F in 10^5 dyn cm^{-1}; H in 10^{-11} erg rad^{-2}. Force constants for bromide and iodide are based on a correction to ref 6. See text. [b] Figures in parentheses are the estimated uncertainties in the parameters. [c] Value obtained by trial and error; fixed in least-squares analysis.

Discussion

The increasing value of K_{PB} along the sequence $BCl_3 < BBr_3 < BI_3$ in both Me_3PBX_3 and PH_3BX_3 follows the increase in acidity of the BX_3 group. Upon adduct formation there is a concurrent reduction in K_{BX} relative to its value in free BX_3 and an increase in f_{CH^2} over free Me_3P. The stiffening of the C–P bond is consistent with a *shortening* of the bond such as has been observed in $Me_3P{\cdot}BH_3$ (1.819 ± 0.010 Å)[30] relative to free Me_3P (1.843 ± 0.003 Å).[29] The similar strengthening of the PH bond in $Me_2HP{\cdot}BH_3$ relative to Me_2PH was previously observed and rationalized in terms of a rehybridization of the phosphorus bonding orbitals upon adduct formation.[32] The C–P bond stiffening and shortening in the Me_3P adduct formation is in contrast to the *weakening* and *lengthening* of the C–N bond observed in Me_3NBX_3[22] and other trimethylamine adducts. The results involving Me_3N as a base do not agree with the valence-shell electron-pair repulsion model. This has been rationalized as arising from the dominance of the repulsion between methyl groups attached to nitrogen.[33] For the larger phosphorus atom, it is not surprising that this repulsion is apparently less significant. Hence the changes in bond distances in these Me_3P species are consistent with the VSEPR model.

Acknowledgment. We wish to thank the National Research Council of Canada for financial support.

Registry No. $Me_3P{\cdot}BCl_3$, 13292-83-6; $Me_3P{\cdot}BBr_3$, 13292-85-8; $Me_3P{\cdot}BI_3$, 54215-81-5; Me_3P, 594-09-2; $PH_3{\cdot}BBr_3$, 16610-73-4; $PH_3{\cdot}BI_3$, 38822-60-5.

Supplementary Material Available: Table II, giving a composite listing of all observed and calculated fundamental frequencies for the adduct series $Me_3P{\cdot}BX_3$, X = Cl, Br, I (2 pages). Ordering information is given on any current masthead page.

References and Notes

(1) Part 8: J. E. Drake and B. Rapp, *J. Inorg. Nucl. Chem.*, **36**, 2613 (1974).
(2) M. A. Frish, H. G. Heal, H. Mackle, and I. O. Madden, *J. Chem. Soc.*, 899 (1965), and references therein.
(3) R. W. Rudolph, R. W. Parry, and C. F. Farran, *Inorg. Chem.*, **5**, 723 (1966).
(4) J. Davis and J. E. Drake, *J. Chem. Soc. A*, 2094 (1971).
(5) J. D. Odom, S. Riethmiller, J. D. Witt, and J. R. Durig, *Inorg. Chem.*, **12**, 1123 (1973).
(6) J. E. Drake, J. L. Hencher, and B. Rapp, *J. Chem. Soc., Dalton Trans.*, 595 (1974).
(7) W. Sawodny and J. Goubeau, *Z. Anorg. Allg. Chem.*, **356**, 289 (1968).
(8) G. W. Chantry, A. Finch, P. N. Gates, and D. Steele, *J. Chem. Soc. A*, 896 (1966).

(9) J. R. Durig, S. Riethmiller, V. F. Kalinsinsky, and J. D. Odom, *Inorg. Chem.*, **13**, 2729 (1974).
(10) B. Rapp and J. E. Drake, *Inorg. Chem.*, **12**, 2868 (1973).
(11) A. H. Cowley and M. C. Damasco, *J. Am. Chem. Soc.*, **93**, 6815 (1971).
(12) R. H. Staley and J. L. Beauchamp, *J. Am. Chem. Soc.*, **96**, 6252 (1974).
(13) R. T. Markham, E. A. Dietz, Jr., and D. R. Martin, *J. Inorg. Nucl. Chem.*, **35**, 2629 (1973).
(14) A. B. Burg and R. I. Wagner, *J. Am. Chem. Soc.*, **75**, 3872 (1953); D. F. Shriver, "The Manipulation of Air-Sensitive Compounds", McGraw-Hill, New York, N.Y., 1969, p 281.
(15) J. F. Nixon and R. Schmutzler, *Spectrochim. Acta*, **22**, 656 (1966).
(16) M. Halmann, *Spectrochim. Acta*, **16**, 407 (1960).
(17) E. J. Rosenbaum, D. J. Rubin, and C. R. Sandberg, *J. Chem. Phys.*, **8**, 366 (1940).
(18) G. Bouquet and M. Bigorgne, *Spectrochim. Acta, Part A*, **23**, 1231 (1967).
(19) J. E. Drake and B. Rapp, *J. Chem. Soc., Dalton Trans.*, 2341 (1972).
(20) Supplementary material.
(21) J. D. Odom, B. A. Hudgens, and J. R. Durig, *J. Phys. Chem.*, **16**, 1972 (1973).
(22) P. D. H. Clippard, Ph.D. Thesis, University of Michigan, 1969.
(23) D. F. Shriver and B. Swanson, *Inorg. Chem.*, **10**, 1354 (1971).
(24) R. I. Amster and R. C. Taylor, *Spectrochim. Acta*, **20**, 1487 (1964).
(25) T. Wentick and V. H. Tiensu, *J. Chem. Phys.*, **28**, 826 (1958).
(26) G. Herzberg, "Molecular Spectra and Molecular Structure", Vol. II, Van Nostrand, Princeton, N.J., 1968, p 491.
(27) J. L. Hencher, Ph.D. Thesis, McMaster University, 1965.
(28) W. D. Gwinn, *J. Chem. Phys.*, **55**, 417 (1971).
(29) L. S. Bartell and L. O. Brockway, *J. Chem. Phys.*, **32**, 512 (1960); P. S. Bryan and R. L. Kuczkowski, *ibid.*, **55**, 3049 (1971).
(30) P. S. Bryan and R. L. Kuczkowski, *Inorg. Chem.*, **11**, 553 (1972).
(31) T. Shimanouchi, "Physical Chemistry: An Advanced Treatise", Vol. IV, D. Henderson, Ed., Academic Press, New York, N.Y., 1970, p 233.
(32) A. B. Burg, *Inorg. Chem.*, **3**, 1325 (1964).
(33) A. Haaland, *Top. Curr. Chem.*, **53**, 11–13 (1975).

Contribution from the Department of Chemistry, University of Massachusetts, Amherst, Massachusetts 01003

Crystal and Molecular Structure of the Spirophosphorane $(C_6H_4O_2)_2PCl$[1]

RICHARD K. BROWN[2] and ROBERT R. HOLMES*

Received December 13, 1976 AIC608845

The crystal structure of 2-chloro-2,2′-spirobis(1,3,2-benzodioxaphosphole), $(C_6H_4O_2)_2PCl$, has been determined by single-crystal x-ray diffraction analysis. The compound crystallizes in the monoclinic space group, $P2_1/n$, with cell constants $a = 6.748$ (6) Å, $b = 12.638$ (8) Å, $c = 14.229$ (9) Å, $\beta = 76.19$ (5)°, and $Z = 4$. The molecule contains a noncrystallographic twofold axis about the P–Cl bond. With reference to the Berry coordinate, the geometry about phosphorus is 72% displaced from a trigonal bipyramid (TP) toward a rectangular pyramid (RP). Pertinent features of the molecule are the diagonal O–P–O angles, 162.9 (1) and 149.8 (1)°, and the four bond angles between the axial chlorine atom and the basal P–O bonds, 105.0 (1), 98.3 (1), 98.8 (1), and 105.3 (1)°. The differences in the basal P–O bond lengths, 1.643 (3) and 1.640 (3) vs. 1.657 (3) and 1.662 (3) Å, are indicative of small residual trigonal-bipyramidal character. The phosphorus atom is 0.338 Å out of the mean plane of the four oxygen atoms toward the axial chlorine atom. The structure is discussed with respect to its position in the series of related substances, $(C_6H_4O_2)_2PR$ (R = F, Cl, Ph, adamantyl, CH_3, and OPh), and comparisons are made with the structures of $(CF_3)_2PCl_3$ and $(CF_3)_3PCl_2$.

Introduction

Interesting five-coordinate cyclic phosphorane structures have recently been established by x-ray crystallography.[3-19] Among these are I–VI shown below. The conformations of I, II, and V show relatively modest structural deviations from a rectangular pyramid (RP) while the conformations of III, IV, and VI are best viewed in terms of some degree of structural variation from the idealized trigonal bipyramid (TP).[20a] For the five-membered cyclic derivatives, the Berry coordinate[21] accurately reflects the type of structural distortion encountered.[20]

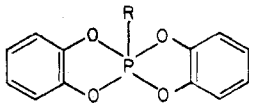

I, R = Me,[4b] OPh,[8] Ad,[16] Ph,[5] Fe[4c] (Ad = adamantyl)

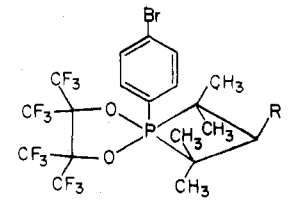

II,[19] R = H, CH_3

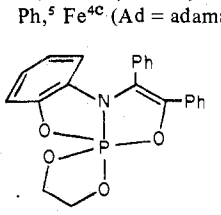

III[15]

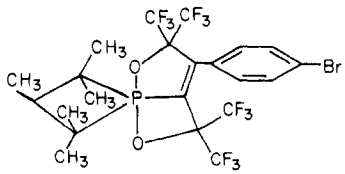

IV[18]

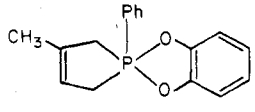

V[3a]

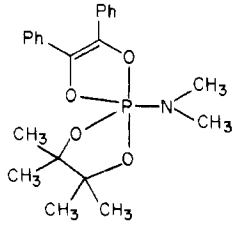

VI[3b]

Factors important in influencing the observed structural variations have been discussed[20,22] and serve in an initial attempt to reproduce some of these structures via conformational minimization techniques[1b,23] based on a well-parameterized molecular mechanics model.[1b,23,24] The success in this attempt has led to the application of the computer simulation method to quantitatively delineate the course of the action of ribonuclease on nucleic acid substrates.[25] The latter are postulated to hydrolytically break down by way of phosphorane intermediates.[26]

Examination of the ligand construction for the derivatives I–VI suggests factors that appear dominant in determining the structures of cyclic phosphoranes. Neither carbon or nitrogen, due to the low electronegativity[27] of the former and high equatorial π-bonding characteristics[28] of the latter, prefers to reside in axial positions of a TP. Such factors contribute as structural determinants in II, IV, and V.[22] The presence of ring unsaturation and electron delocalization contribute as factors determining the structures of derivatives of I. Increased ligand electronegativity in III compared to IV and ring constraints of III relative to VI serve to establish the resulting structure of III. When VI is compared to members of I, the influence of ring unsaturation appears contributory in stabilizing the RP.[22]

It is important to assess the comparative role of each of the factors influencing the geometries of cyclic phosphoranes in